Pulse shape influence on the atmospheric barrier discharge

T. Martens,[1,a)] A. Bogaerts,[1] and J. van Dijk[2]
[1]*Department of Chemistry, University of Antwerp, Universiteitsplein 1 B-2610 Antwerp, Belgium*
[2]*Department of Applied Physics, Eindhoven University of Technology, 5600 MB Eindhoven, The Netherlands*

(Received 4 November 2009; accepted 4 January 2010; published online 31 March 2010)

In this letter we compare the effect of a radio-frequency sine, a low frequency sine, a rectangular and a pulsed dc voltage profile on the calculated electron production and power consumption in the dielectric barrier discharge. We also demonstrate using calculated potential distribution profiles of high time and space resolution how the pulsed dc discharge generates a secondary discharge pulse by deactivating the power supply. © *2010 American Institute of Physics*. [doi:10.1063/1.3315881]

The shape of the applied voltage profile is a crucial factor in generating cold atmospheric pressure plasmas.[1] In the present letter we first compare four typical applied voltage profiles and investigate which has the best performance concerning electron production and power consumption. In order to obtain a better understanding of the synergy between the power applied to the electrodes and the energy stored on the surfaces of the dielectric barriers we subsequently study the best performing setup in detail using calculated potential distributions of high time and space resolution.

For the investigation of the atmospheric pressure dielectric barrier discharges (DBDs) we use a two-dimensional fluid model. The model is part of the Plasimo modeling framework[2] and is based on continuity equations for mass, momentum and electron energy, which are numerically solved coupled to the Poisson equation for the electric field. Details on the physical descriptions and the numerical techniques that are being used can be found elsewhere.[3]

The experimental setup under study is a DBD with both electrodes covered with an alumina dielectric ($\epsilon_r = 9$) of 1 mm thickness. The spacing between the dielectric surfaces is 5 mm and on the top electrode a sinusoidal voltage is applied while the bottom electrode is grounded. The operating gas is atmospheric pressure helium with 100 ppm of nitrogen impurity and it is described using nine different species and 18 different chemical reactions, the details of which can be found elsewhere.[4]

The validity of our model for this setup has previously been assessed,[5] where an almost perfect agreement with the results of Luo *et al.*[6] concerning the discharge current and gap voltage characteristics was obtained together with agreement of the spatial evolution of the discharge in time.

In order to obtain a better insight in the electron generation and power consumption costs of different types of applied voltage profiles, four distinct setups were chosen which all interact very differently with the deposited charge on the dielectrics. Figure 1 illustrates the applied voltage and the calculated gap voltage and current density of the four voltage profiles. All setups use a 4 kV peak-to-peak voltage. Setup 1 is a radio-frequency (rf) discharge operating at 13.56 MHz, setup 2 a sinusoidal applied voltage at 10 kHz, setup 3 a rectangular voltage at 10 kHz and setup 4 is a pulsed dc discharge operating at 10 kHz. For the rectangular voltage and the pulsed dc discharge rise times of 50 ns are used. This value is based on the setups of Liu, Laroussi and Lu.[7–9] Note that the difference between setups 3 and 4 is that the rectangular voltage has both positive and negative values, whereas the pulsed dc discharge has only a positive applied voltage.

The rf setup (1) produces a very powerful discharge with a maximum current density of about 300 mA/cm^2. The quenching effect of the charges accumulated on the dielectrics is very limited for this profile, because at such a high frequency the charged species are too much trapped in the discharge to quickly compensate the electric field before the polarity on the powered electrode has changed. As a consequence an almost sinusoidal profile is obtained for the discharge current which is slightly more than one eighth of a period out of phase with the applied voltage.

The 10 kHz sinusoidal voltage (2) is the most typical profile for this kind of setup. It can be seen in Fig. 1 that the gap voltage increases until a value of 1.5 kV is reached and then gas breakdown occurs, whereafter the discharge is quickly quenched again due to the accumulation of charges on the dielectrics. This creates a self-sustained pulsed discharge system, although powered by a continuous sinus,

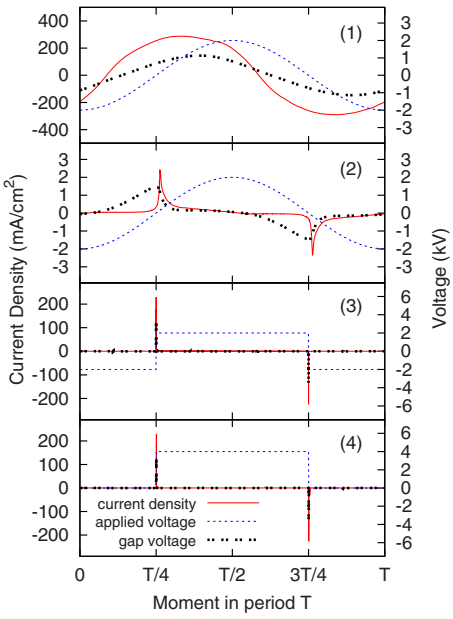

FIG. 1. (Color online) Current density, gap voltage, and applied voltage during one period of applied voltage. Setup (1) uses a rf voltage, (2) a 10 kHz sinusoidal profile, (3) a rectangular voltage, and (4) a pulsed dc profile.

a)Author to whom correspondence should be addressed. Electronic mail: tom.martens@ua.ac.be.

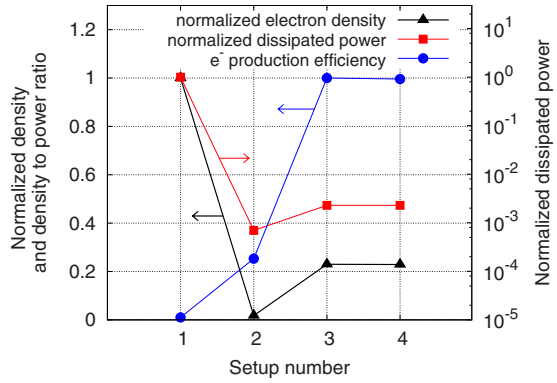

FIG. 2. (Color online) Normalized electron density, plasma power, and e^- production efficiency for the rf voltage (1), the 10 kHz sinusoidal voltage (2), rectangular (3), and pulsed dc voltage (4).

which is low in power consumption because it is a short current pulse, with an amplitude 100 times smaller than for the rf discharge.[10]

Figure 1 demonstrates that generating a DBD plasma with a rectangular voltage (3) or with a pulsed dc profile (4) using frequencies of 10 kHz and peak-to-peak voltages of 4 kV generates the same plasma which exhibits a current pulse of 230 $\mathrm{mA/cm^2}$ right after a gap voltage of 3.4 kV is reached.

In order to assess the use of the different types of power supply an estimation for the power consumption is needed. The time averaged power dissipated in the discharge can be determined by $\langle P_{\mathrm{diss}}\rangle=(\int_T P_{\mathrm{diss}}dt)/(\int_T dt)$ where T is the length of one period and P_{diss} is the dissipated power determined by $P_{\mathrm{diss}}=(\int_{\mathrm{vol}}\vec{J}\cdot\vec{E}dV)/(\int_{\mathrm{vol}}dV)$, which is an integration over the volume of the product of plasma current density and electric field.

The calculated dissipated power of the 4 setups is plotted in Fig. 2 together with the time and space averaged electron density, as well as the ratio of this electron density to the dissipated power in order to obtain an idea of electron production efficiency. Since the focus lies on the comparison between the setups and in order to show all information in one plot, all values in Fig. 2 are normalized to their highest value. The electron density and the electron production efficiency are plotted to the linear axis on the left, while the dissipated power is plotted to the logarithmic axis on the right.

Figure 2 demonstrates that the rf discharge (1) very clearly has the highest electron production, but requires an enormous amount of power. Due to this high power consumption, the rf discharge clearly has the lowest efficiency in the electron production. The other three setups all give rise to a discharge pulsed in nature, which can be seen in Fig. 1. Since the current in a pulsed discharge only flows for a limited amount of time, also the power consumption is limited in time. As a consequence, the dissipated power of setups 2, 3, and 4 is almost three orders of magnitude lower than for setup 1, as is illustrated in Fig. 2.

Figure 2 also shows that the efficiency of the rectangular profiles (3) and (4) is about four times higher than the sinusoidal profile. This increased efficiency is obtained because the rectangular voltage (3) and the pulsed dc voltage (4) are characterized by a change in the applied voltage on the electrodes during only 50 ns in half a period, which makes 100 ns in an entire period. A change of 4 kV during 50 ns provides for a voltage growth rate of 8×10^{10} $\mathrm{V\,s^{-1}}$. This is about 300 times higher than the voltage growth rate at the point of breakdown when using a sinusoidal profile with an amplitude of 4 kV and a frequency of 10 kHz, i.e., 2.5×10^8 $\mathrm{V\,s^{-1}}$. Increasing the voltage growth rate in an atmospheric pressure DBD significantly increases the maximal current density and the space charge.[11] Therefore, the rectangular profile (3) and the pulsed dc voltage (4) provide for a much higher electron density than the sinusoidal voltage (2), as can be seen in Fig. 2. Figure 2 also demonstrates that the increased pulse strength requires a greater amount of power, but the increased demand of power remains limited because the discharge pulse lasts only for 150 ns, while for the sinusoidal profile the discharge pulse lasts for 6.05 μs, which is about 40 times longer. Therefore, the increased voltage growth rate, which causes the discharge pulse to be stronger, in combination with the restricted pulse width, which causes the power consumption to be limited in time, are responsible for the superior efficiency of the rectangular voltage (3) and the pulsed dc voltage (4).

Figure 2 illustrates that the same results are obtained for the rectangular voltage (3) and the pulsed dc discharge (4). It is logical that the same discharge is obtained when the same peak-to-peak voltage is used in a DBD, because as can be seen in Fig. 1 due to the charge accumulation on the dielectrics, the same gap voltages are obtained. The real power consumption, however, will be different. Our model describes only the dissipated power calculated from the equations mentioned above. In order to obtain a full estimation of the power consumption, the supplied power needs to be calculated, i.e., $P_{\mathrm{supp}}=(\int_{\mathrm{vol}}I_{\mathrm{total}}\cdot\phi_{\mathrm{app}}dV)/(\int_{\mathrm{vol}}dV)$, where I_{total} is the total electric current and ϕ_{app} is the applied potential.[8] The total electric current comprises the discharge current as well as the external current flowing through the electrical circuit. Hence to calculate the latter, a description of the electrical circuit is needed and this is currently not yet present in our model. An estimation, however, can be made, because the total current and the discharge current will always possess the same positive or negative sign.[8] Figure 1 demonstrates that for both setup 3 and 4 one positive and one negative current pulse is obtained within one period. The most important difference between setup 3 and 4 is that the rectangular applied voltage (3) has both positive and negative values, whereas the pulsed dc discharge (4) has only a positive applied voltage. Hence, for the rectangular voltage the supplied power in one period is determined by first a product of positive current and positive voltage and second by a product of negative current and negative voltage (setup 3, Fig. 1). Therefore, it gives twice a positive contribution for the supplied power. For the pulsed dc voltage, on the other hand, the supplied power in one period is determined by first a product of a positive current and a positive applied voltage and second by a product of a negative current and a positive voltage very quickly going to zero (setup 4, Fig. 1). Therefore, it is first a positive value, but the second contribution is a small negative value, because the second discharge pulse is generated simply by turning the power source off. This small negative value provides for a so-called power recuperation effect,[8] which will always make the power consumption of the pulsed dc discharge (4) lower than for the rectangular voltage (3). Therefore, of all studied profiles the pulsed dc

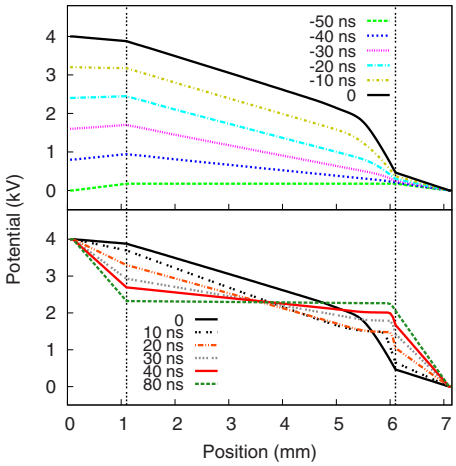

FIG. 3. (Color online) Spatial profiles of the electric potential from the powered electrode on the left to the grounded electrode on the right. The vertical lines illustrate the surfaces of the dielectrics on the electrodes. The profiles are shown from 50 ns before the maximum gap voltage of 3.4 kV is reached (0), until 80 ns after the maximum gap voltage.

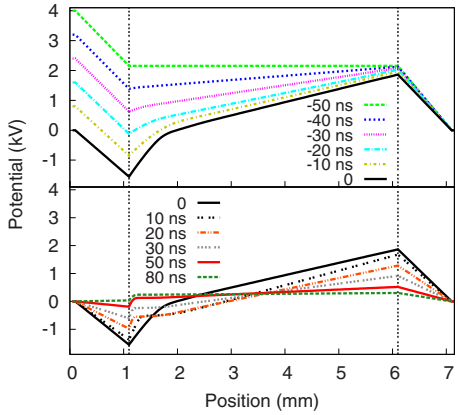

FIG. 4. (Color online) Similar profiles as in Fig. 3. The profiles are shown from 50 ns before the minimum gap voltage of −3.4 kV is reached (0), until 80 ns after the minimum gap voltage. Note that the dashed line at −50 ns in the upper frame has exactly the same shape as the dashed line at 80 ns in the bottom frame of Fig. 3, demonstrating that the potential distribution does not change for about 50 μs between the times of maximum and minimum gap voltage.

discharge will have the highest electron generation efficiency.

These efficiency calculations were also carried out for the electron energy density, because it is a combination of the energy used in order to generate electrons and the energy that is used to heat up the electrons. Using this parameter to assess the efficiency gave the same results.

The discharge pulse formations due to power activation and deactivation are studied by means of calculated potential distribution profiles of very high time and space resolution. The spatial emission behavior during these breakdown phenomena has been captured by Lu and Laroussi[12] by using high speed imaging. The images showed that for the first breakdown the plasma emission starts in the bulk region, while for the second breakdown this emission starts at the momentary anode and then moves toward the cathode. In this letter we illustrate in Figs. 3 and 4 the calculated spatial profiles of the electric potential throughout the discharge, including the dielectrics and electrodes. The powered electrode is on the left and the grounded electrode is on the right. In the top frame of Fig. 3 the transition is shown from zero gap voltage (−50 ns) evolving in six steps to maximum gap voltage (0). At that point there is breakdown in the gas and 20 ns later the maximum current density is reached. This very quick uprise in both current and charge density causes the ionized gas to charge both dielectrics. The latter compensates the potential difference between the electrodes so that the gap voltage gradually becomes zero again. The compensation of applied voltages by the surface charges is shown in the bottom frame of Fig. 3 in six consecutive profiles. Here it can be seen that although the potential difference between the electrodes is 4 kV, the difference between the dielectric surfaces becomes negligible within 80 ns. Afterwards a potential of about 2.2 kV is upheld at both dielectrics during 50 μs. This is the potential energy that is stored on the surfaces.

Indeed, the potential distribution illustrated by the last profile in Fig. 3, at 80 ns after the maximum gap voltage, barely changes for about 50 μs. Therefore, the difference with the first profile in Fig. 4, at 50 ns before the minimum gap voltage, is negligible. Figure 4 clarifies the creation of the secondary pulse. When the applied potential is set to zero on the powered electrode, the decrease of this potential pushes the potential on the adjacent dielectric downwards. Since there are still charges stored on the dielectric, the potential is pushed far below zero until a value of −1.3 kV is reached. The other electrode is grounded and therefore not much happens on the adjacent dielectric on whose surface a potential of about 2 kV is upheld. This creates a very large gap voltage and a second breakdown occurs. Hence, this explains the responsible mechanism for the secondary discharge pulse by deactivating the power supply. This mechanism can be followed in Fig. 4 where, similar as in Fig. 3, the spatial potential profiles are plotted. The top frame shows the profiles from zero gap voltage (−50 ns) to maximum gap voltage (0) in six steps and the bottom frame illustrates the similar evolution from maximum gap voltage to a negligible gap voltage.

[1]M. G. Kong and X. T. Deng, IEEE Trans. Plasma Sci. **31**, 7 (2003).
[2]J. van Dijk, K. Peerenboom, M. Jimenez, D. Mihailova, and J. van der Mullen, J. Phys. D **42**, 194012 (2009).
[3]G. Hagelaar, Ph.D. thesis, TU/e Eindhoven, 2000.
[4]T. Martens, A. Bogaerts, W. J. M. Brok, and J. v Dijk, Appl. Phys. Lett. **92**, 041504 (2008).
[5]T. Martens, W. J. M. Brok, J. van Dijk, and A. Bogaerts, J. Phys. D **42**, 122002 (2009).
[6]H. Luo, Z. Liang, B. Lv, X. Wang, Z. Guan, and L. Wang, Appl. Phys. Lett. **91**, 221504 (2007).
[7]S. Liu and M. Neiger, J. Phys. D **34**, 1632 (2001).
[8]M. Laroussi, X. Lu, V. Kolobov, and R. Arslanbekov, J. Appl. Phys. **96**, 3028 (2004).
[9]X. Lu and M. Laroussi, J. Appl. Phys. **98**, 023301 (2005).
[10]G. E. Georghiou, A. P. Papadakis, R. Morrow, and A. C. Metaxas, J. Phys. D **38**, R303 (2005).
[11]Y. B. Golubovskii, V. A. Maiorov, J. Behnke, and J. F. Behnke, J. Phys. D **36**, 975 (2003).
[12]X. P. Lu and M. Laroussi, J. Phys. D **39**, 1127 (2006).